Effects of a finite number of particles on the thermodynamic properties of a harmonically trapped ideal charged Bose gas in a constant magnetic field*

Duan-Liang Xiao(肖端亮), Meng-Yun Lai(赖梦云), and Xiao-Yin Pan(潘孝胤)†

Department of Physics, Ningbo University, Ningbo 315211, *China*

(Received 22 June 2015; revised manuscript received 10 September 2015; published online 30 November 2015)

We investigate the thermodynamic properties of an ideal charged Bose gas confined in an anisotropic harmonic potential and a constant magnetic field. Using an accurate density of states, we calculate analytically the thermodynamic potential and consequently various intriguing thermodynamic properties, including the Bose–Einstein transition temperature, the specific heat, magnetization, and the corrections to these quantities due to the finite number of particles are also given explicitly. In contrast to the infinite number of particles scenarios, we show that those thermodynamic properties, particularly the Bose–Einstein transition temperature depends upon the strength of the magnetic field due to the finiteness of the particle numbers, and the collective effects of a finite number of particles become larger when the particle number decreases. Moreover, the magnetization varies with the temperature due to the finiteness of the particle number while it keeps invariant in the thermodynamic limit $N \to \infty$.

Keywords: Bose–Einstein condensation, thermodynamic potential, specific heat, magnetization

PACS: 03.75.Hh, 05.30.Jp, 75.20.–g **DOI:** 10.1088/1674-1056/25/1/010307

1. Introduction

The ideal charged Bose gas (CBG) consists of a gas of spin-less, charged bosons coupled to an external homogeneous magnetic field has played a significant role in understanding lots of exotic quantum phenomena including superfluidity and superconductivity. The study of the CBG has a long history and it is impossible to give a complete list here. Perhaps, the first investigation in three dimensions was performed more than half a century ago by Osboren,[1] and then by Schafroth[2] who showed that Bose–Einstein condensation (BEC)[3–7] cannot exist at any finite temperature in the presence of a homogeneous magnetic field. However, the system does exhibit the essential equilibrium features of a superconductor such as the Meissner–Ochsenfeld (MO) effect at lower temperatures in a magnetic field. May[8,9] extended this idea to a D-dimensional CBG and pointed out the BEC in CBG can take place only if $D \geq 5$. Toms[10,11] subsequently argued that BEC cannot occur in the CGB in any spatial dimension D, while Rojas[12] has pointed out that BEC can take place with a diffuse transition. May's work was confirmed and extended by Daicic and Frankel.[13] A semiclassical approach was used by Bayindir and Tanatar[14] to conclude that BEC can occur in the CBG in a magnetic field and in the presence of a crossed electric field. The thermodynamic properties of the 2D CBG in a magnetic field has also been investigated by van Zyl and Hutchinson.[15]

In recent years, with rapid progress in ultracold atoms, there has been a renewed interest in charged bosons. In a properly designed laser field, the center-of-mass (CM) motion of neutral atoms may mimic the dynamics of a charged particle in a magnetic field.[16] Alternatively, one can spin up the neutral atoms by confining them in a rotating frame.[17] Since the atomic gases of the experiments for BEC are dilute, as a first approximation the ideal Bose gas is a good starting model to explore theoretically in terms of basic interatomic interactions. Although not the focus of rotating Bose gases research, the thermodynamic properties of the rotating ideal Bose gases have also been studied by various authors.[18–23] In particular, the ideal CGB in a magnetic field was taken as an example to investigate the thermodynamic properties of rotating ideal Bose gases by the authors of Ref. [24]. The system they considered is placed in a uniform magnetic field and a harmonic trap

$$V = \frac{m}{2}(\omega^2 x^2 + \omega^2 y^2 + \omega_z^2 z^2). \tag{1}$$

Based on the thermodynamic limit approximation, i.e., the particle number is infinite, they found that the BEC condensation temperature is irrelevant to the magnetic field, which is conflicting with established intuition that the critical temperature decreases when the strength of the magnetic field increases.

However, it is well known that in real experiment conditions, the number of trapped atoms N is finite ranging from a few thousand[25] to a few million,[26] the thermodynamic limit approximation may not be available. Actually, there are quite a lot of works dealing with this issue for the Bose gases.[27–35]

*Project supported by the National Natural Science Foundation of China (Grant No. 11375090), and the K. C. Wong Magna Foundation of Ningbo University, China.

†Corresponding author. E-mail: panxiaoyin@nbu.edu.cn

© 2016 Chinese Physical Society and IOP Publishing Ltd

Hence, in this paper we investigate the effects of a finite number of particles on the thermodynamic properties of an ideal charged Bose gas confined in an anisotropic harmonic potential and a constant magnetic field. Using an accurate density of states, we first calculate analytically the thermodynamic potential, then various thermodynamic properties including the Bose–Einstein transition temperature, the specific heat, and magnetization are analyzed. The corrections to these quantities due to the effects of a finite number of particles are also given explicitly. In particular, we show that the BEC condensation temperature is relevant to the magnetic field and the magnetization varies with the temperature when the particle number is finite. These behaviors are quite different from the infinite particle number case.

The rest of the paper is organized as follows. In Section 2, we introduce the Hamiltonian of the system and give the energy spectrum. The thermodynamic potential and various thermodynamic potentials are obtained and analyzed in Section 3, concluding remarks are made in the last section.

2. Hamiltonian and energy spectrum

The ideal charged Bose gas we consider consists of N bosons with mass m and charge $e>0$, is trapped in a harmonic confining potential which is anisotropic in all three dimensions[26,36] described by

$$V_{\rm trap}=\frac{m}{2}(\omega_x^2x^2+\omega_y^2y^2+\omega_z^2z^2), \tag{2}$$

and also is under a perpendicular magnetic field B in the z direction. Choosing a symmetric gauge $\boldsymbol{A}=\boldsymbol{B}\times\boldsymbol{r}/2=(-By/2,Bx/2,0)$, we have the Hamiltonian

$$H=\frac{\left(p_x-\frac{q}{c}A_x\right)^2}{2m}+\frac{\left(p_y-\frac{q}{c}A_y\right)^2}{2m}+V_{\rm trap}, \tag{3}$$

where c is the speed of light and $q=e$ is the charge. The Hamiltonian can be decomposed into two parts

$$H=H_{xy}+H_z, \tag{4}$$

where $H_z=p_z^2/2m+m\omega_z^2z^2/2$ describing the z direction with trap frequency ω_z and eigenvalues $E_{n_3}=(n_3+1/2)\hbar\omega_z$, and

$$H_{xy}=\frac{1}{2m}(p_x^2+p_y^2)+\frac{1}{2m}(\tilde{\omega}_x^2x^2+\tilde{\omega}_y^2y^2)+\frac{\omega_{\rm c}}{2}L_z \tag{5}$$

describes the in-plane motion with

$$\tilde{\omega}_x=\sqrt{\omega_x^2+\frac{\omega_{\rm c}^2}{4}},\quad \tilde{\omega}_y=\sqrt{\omega_y^2+\frac{\omega_{\rm c}^2}{4}},$$

and $\omega_{\rm c}=qB/(mc)$, the cyclotron frequency. Without loss of generality, we may assume $\omega_x\leq\omega_y$. The energy levels for H_{xy} are[37]

$$E_{n_1n_2}=\left(n_1+\frac{1}{2}\right)\hbar\omega_1+\left(n_2+\frac{1}{2}\right)\hbar\omega_2, \tag{6}$$

where

$$\omega_{2,1}=\frac{1}{\sqrt{2}}\Big\{\omega_x^2+\omega_y^2+\omega_{\rm c}^2 \pm\sqrt{(\omega_x^2+\omega_y^2+\omega_{\rm c}^2)^2-4\omega_x^2\omega_y^2}\Big\}^{1/2}. \tag{7}$$

The corresponding eigenfunctions for the Hamiltonian of Eq. (5) are also known, we refer the reader to Ref. [37] for more details. The behaviors of the frequencies $\omega_{2,1}$ as functions of the strength of magnetic field B are plotted in Fig. 1. In the case of isotropic harmonic potential, i.e., $\omega_x=\omega_y=\omega_0$, then $\omega_{1,2}=\omega\mp\omega_{\rm c}/2$ with $\omega=\sqrt{\omega_0^2+\omega_{\rm c}^2/4}$. In Fig. 2, we plot the in-plane energy levels $E_{n_1n_2}$ as a function of the cyclotron frequency $\omega_{\rm c}=eB/(mc)$.

Hence, the energy levels of the total model Hamiltonian are

$$\begin{aligned}E_{n_1n_2n_3}&=\left(n_1+\frac{1}{2}\right)\hbar\omega_1+\left(n_2+\frac{1}{2}\right)\hbar\omega_2+\left(n_3+\frac{1}{2}\right)\hbar\omega_z\\&=\epsilon_{n_1n_2n_3}+E_0,\end{aligned} \tag{8}$$

where $\epsilon_{n_1n_2n_3}=n_1\hbar\omega_1+n_2\hbar\omega_2+n_3\hbar\omega_z$, and $E_0=\hbar(\omega_1+\omega_2+\omega_z)/2$ is the ground state energy.

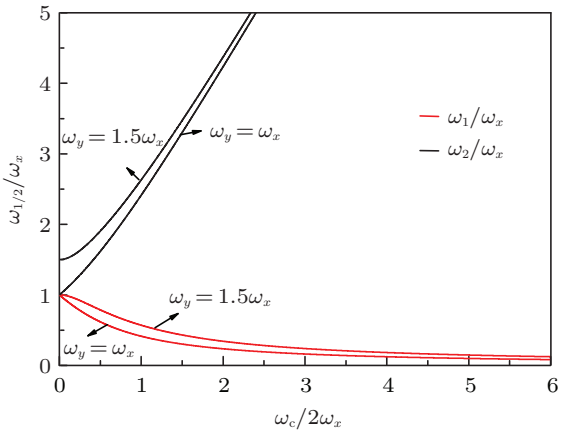


Fig. 1. (color online) The $\omega_{1,2}/\omega_x$ as functions of the cyclotron frequency $\omega_{\rm c}=eB/(mc)$ (in units of $2\omega_x$), which is proportional to the strength of the magnetic field B.

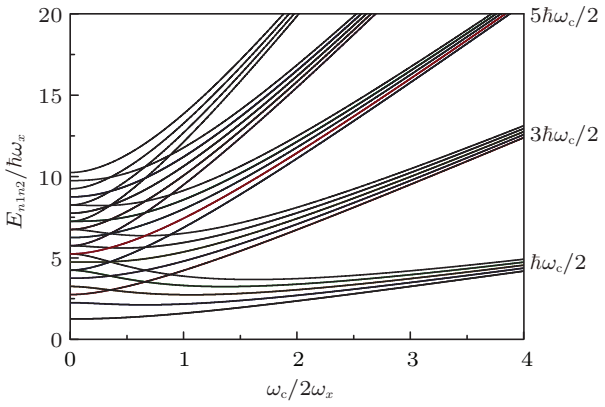


Fig. 2. (color online) The in-plane energy levels $E_{n_1n_2}$ (in units of $\hbar\omega_x$) as functions of the cyclotron frequency $\omega_{\rm c}=eB/(mc)$ (in units of $2\omega_x$), which is proportional to the strength of the magnetic field B.

3. Thermodynamic properties

In this section, we first calculate the thermodynamic potential, then the transition temperature and condensate fraction are obtained by taking into account the fact that the particle number N is finite. Finally, we calculate the specific heat and magnetization.

3.1. Thermodynamic potential

The thermodynamic potential of the system is[38]

$$\begin{aligned}\Omega &= \frac{1}{\beta}\sum_{\{n_1n_2n_z\}}\ln(1-\mathrm{e}^{-\beta(E_{n_1n_2n_z}-\mu)})\\ &= \frac{1}{\beta}\sum_{\{n_1n_2n_z\}}\ln(1-z\mathrm{e}^{-\beta\epsilon_{n_1n_2n_z}}),\end{aligned} \tag{9}$$

where $\beta=(k_{\mathrm{B}}T)^{-1}$ is the inverse temperature, $z=\mathrm{e}^{\beta(\mu-E_0)}$. The above expression usually can be written as two parts

$$\Omega=\Omega_0+\Omega_{T\neq0}, \tag{10}$$

where the first part $\Omega_0=\ln(1-z)/\beta$, which is present only when there is a nonzero condensate. Alternatively, this part can also be described by using a background field $\Psi(\boldsymbol{r})$,[39,40]

$$\Omega_0=\int \mathrm{d}^3\boldsymbol{r}\left(\frac{|\mathscr{D}\Psi|^2}{2m}+V_{\mathrm{trap}}(\boldsymbol{r})|\Psi|^2-\mu|\Psi|^2\right). \tag{11}$$

Notice here $\mathscr{D}\Psi=\mathrm{i}(\boldsymbol{P}-q\boldsymbol{A}/c)\Psi$ is the gauge-covariant derivative. The nonzero value of the background field Ψ which signals a condensate satisfies the following equation:

$$\frac{1}{2m}\mathscr{D}^2\Psi-V_{\mathrm{trap}}(\boldsymbol{r})\Psi+\mu|\Psi|=0. \tag{12}$$

Thus we can expand $\Psi(\boldsymbol{r})$ as $\Psi(\boldsymbol{r})=\sum_n C_n\Psi_n(\boldsymbol{r})$, where $\Psi_n(\boldsymbol{r})$ are stationary state solutions to the Schrödinger equation

$$-\frac{1}{2m}\mathscr{D}^2\Psi_n(\boldsymbol{r})+V_{\mathrm{trap}}(\boldsymbol{r})\Psi_n(\boldsymbol{r})=E_n\Psi_n(\boldsymbol{r}), \tag{13}$$

and they form a complete set. Since equation (13) is exactly the Schrödinger equation for the Hamiltonian of Eq. (4), one immediately realizes that E_n coincides with the single particle energy $E_{n_1n_2n_3}$ of Eq. (8) with $n=\{n_1n_2n_3\}$. The corresponding eigenfunctions are also readily identified as

$$\Psi_{n=\{n_1n_2n_3\}}(\boldsymbol{r})=\Phi_{n_1n_2}(x,y)\phi_{n_3}(z). \tag{14}$$

The coefficients C_n are determined by

$$(E_n-\mu)C_n=0. \tag{15}$$

When the temperature is above the BEC temperature T_{c}, the chemical potential μ is less than the ground state energy, $\mu<E_0$. Thus, $E_n-\mu\neq0$ and $C_n=0$ for all levels. As the temperature decreases, the chemical potential μ increases and reaches E_0 at or below T_{c}. Then $C_0\neq0$ becomes the only nonzero solution of all C_n, which means the corresponding condensate wave function is $\Psi(\boldsymbol{r})=C_0\Psi_0(\boldsymbol{r})$, with

$$\Psi_0(\boldsymbol{r})=\Phi_{00}(x,y)\phi_0(z), \tag{16}$$

where $\Phi_{00}(x,y)$ is the ground state wave function for H_{xy},[37]

$$\Phi_{00}(x,y)=\frac{1}{\pi}\left[\frac{\sqrt{M_1\omega_1M_2\omega_2}}{(\alpha_2^2M_1\omega_1M_2\omega_2+1)}\right]^{1/2}\exp\left[\mathrm{i}\alpha_1xy-\frac{M_1\omega_1x^2+2\mathrm{i}\alpha_2M_1\omega_1M_2\omega_2xy+M_2\omega_2y^2}{2(\alpha_2^2M_1\omega_1M_2\omega_2+1)}\right], \tag{17}$$

with

$$\alpha_1=\frac{m}{2}\left(\frac{\omega_x^2-\omega_y^2}{\omega_{\mathrm{c}}}\right)-\frac{m}{2\omega_{\mathrm{c}}}\sqrt{(\omega_x^2+\omega_y^2+\omega_{\mathrm{c}}^2)^2-4\omega_x^2\omega_y^2}, \tag{18}$$

$$\alpha_2=-\frac{\omega_{\mathrm{c}}}{m\sqrt{(\omega_x^2+\omega_y^2+\omega_{\mathrm{c}}^2)^2-4\omega_x^2\omega_y^2}}, \tag{19}$$

and

$$\begin{aligned}F&=\frac{\sqrt{M_1\omega_1}(x+\mathrm{i}\beta M_2\omega_2y)}{\beta^2M_1\omega_1M_2\omega_2+1},\\ H&=\frac{\sqrt{M_2\omega_2}(\beta M_1\omega_1x-\mathrm{i}y)}{\beta^2M_1\omega_1M_2\omega_2+1},\\ M_{1,2}&=\frac{2m\sqrt{(\omega_x^2+\omega_y^2+\omega_{\mathrm{c}}^2)^2-4\omega_x^2\omega_y^2}}{\sqrt{(\omega_x^2+\omega_y^2+\omega_{\mathrm{c}}^2)^2-4\omega_x^2\omega_y^2}-(\omega_x^2-\omega_y^2\pm\omega_{\mathrm{c}}^2)}.\end{aligned} \tag{20,21}$$

The second part of the thermodynamic potential is

$$\Omega_{T\neq0}=\frac{1}{\beta}\sum_{\{n_1n_2n_z\}}{}'\ln(1-z\mathrm{e}^{-\beta\epsilon_{n_1n_2n_z}}), \tag{22}$$

where $\sum'_{\{n_1n_2n_z\}}$ denotes the summation over all the eigenstates except the ground state. After expanding the logarithm, equation (22) can be expressed as a sum over the Bose–Einstein distribution function as

$$\begin{aligned}\Omega_{T\neq0}&=-\frac{1}{\beta}\sum{}'_{n_1n_2n_3}\frac{z\mathrm{e}^{-\beta\epsilon_n}}{1-z\mathrm{e}^{-\beta\epsilon_n}}\\ &=-\frac{1}{\beta}\sum_{j=1}^{\infty}\frac{z^j}{j!}\int_0^{\infty}g(\epsilon)\mathrm{e}^{-\mathrm{j}\beta\epsilon}\mathrm{d}\epsilon,\end{aligned} \tag{23}$$

where $g(\epsilon)=\sum_{n_1n_2n_3}\delta(\epsilon-\epsilon_{n_1n_2n_3})$ is the density of the states (DOS). In the following we adopt an approximate but very ac-

curate expression for the DOS as in Refs. [27] and [29]

$$g(\epsilon) \approx \frac{1}{2}\frac{\epsilon^2}{(\hbar\bar{\omega}_{\rm g})^3} + \gamma\frac{\epsilon}{(\hbar\bar{\omega}_{\rm g})^2}, \tag{24}$$

where $\bar{\omega}_{\rm g} = (\omega_1\omega_2\omega_z)^{1/3} = (\omega_x\omega_y\omega_z)^{1/3}$, and $\gamma = 3\bar{\omega}/(2\bar{\omega}_{\rm g})$ with $\bar{\omega} = (\omega_1+\omega_2+\omega_z)/3$. Note that γ is a function of B even in the isotropic case. Inserting Eq. (24) into Eq. (23) yields

$$\Omega_{T\neq 0} = -\frac{1}{\beta}\left[\frac{(k_{\rm B}T)^3}{(\hbar\bar{\omega}_{\rm g})^3}g_4(z) + \gamma\frac{(k_{\rm B}T)^2}{(\hbar\bar{\omega}_{\rm g})^2}g_3(z)\right], \tag{25}$$

where $g_k(z) = \sum_{j=1}^{\infty} z^j/j^k$ is the usual Bose–Einstein function.[36]

3.2. Transition temperature and condensate fraction

Having obtained the analytical expression for the thermodynamic potential in the above subsection, we next proceed to calculate the expression for the particle number N which can be derived via the equation $N = -\partial\Omega/\partial\mu$. The transition temperature and condensate fraction then can be obtained from the equation for the particle number.

Employing Eqs. (10) and (25), we can express the particle number as the summation of two parts

$$N = N_0 + N_{\rm e}, \tag{26}$$

where

$$N_0 = -\frac{\partial\Omega_0}{\partial\mu} = \frac{z}{1-z} = |C_0|^2 \tag{27}$$

is the number of particles condensed on the ground state which is nonzero only when the temperature is lower than the transition temperature $T \leq T_{\rm c}$, and

$$N_{\rm e} = -\frac{\partial\Omega_T}{\partial\mu} = \frac{(k_{\rm B}T)^3}{(\hbar\bar{\omega}_{\rm g})^3}g_3(z) + \gamma\frac{(k_{\rm B}T)^2}{(\hbar\bar{\omega}_{\rm g})^2}g_2(z) \tag{28}$$

is the particle number in the excited states.

When $T = T_{\rm c}$, the number of particles condensed on the ground state is pretty large $N_0 \gg 1$ but still $N_0 \ll N$. Hence we can ignore N_0 in Eq. (26) and from Eq. (27) we have $z = N_0/(N_0+1) \approx 1$, consequently we have

$$N \approx \left(\frac{k_{\rm B}T_{\rm c}}{\hbar\bar{\omega}_{\rm g}}\right)^3\zeta(3) + \gamma\left(\frac{k_{\rm B}T_{\rm c}}{\hbar\bar{\omega}_{\rm g}}\right)^2\zeta(2), \tag{29}$$

where $\zeta(n) = g_n(1)$ is the Riemann zeta function. The above equation can be readily solved and we obtain the transition temperature as

$$T_{\rm c} \approx \frac{\hbar\bar{\omega}_{\rm g}}{k_{\rm B}}\left(\frac{N}{\zeta(3)}\right)^{1/3}\left[1 - \frac{\gamma}{3}\frac{\zeta(2)}{\zeta(3)^{2/3}}N^{-1/3}\right]. \tag{30}$$

Note here, in the thermodynamic limit, the second term in the bracket of Eq. (30) can be dropped and the transition temperature becomes

$$T_0 = \frac{\hbar\bar{\omega}_{\rm g}}{k_{\rm B}}\left(\frac{N}{\zeta(3)}\right)^{1/3} \approx 0.94\frac{\hbar\bar{\omega}_{\rm g}}{k_{\rm B}}N^{1/3}, \tag{31}$$

which is irrelevant to the strength of the magnetic field. It should be pointed out that the transition temperature obtained in Ref. [24] is just Eq. (31). Hence, clearly they have taken the thermodynamic limit $N \to \infty$.

Combining Eqs. (30) and (31), we have

$$\begin{aligned}\frac{T_{\rm c}-T_0}{T_0} &\approx -\frac{\gamma}{3}\frac{\zeta(2)}{\zeta(3)^{2/3}}N^{-1/3} \\ &\approx -0.243\left[\frac{\omega_1+\omega_2+\omega_z}{(\omega_x\omega_y\omega_z)^{1/3}}\right]N^{-1/3}.\end{aligned} \tag{32}$$

We plot the ratio $(T_{\rm c}-T_0)/T_0$ as a function of the strength of the magnetic field B in Fig. 3. It is clear from the graph that the ratio decreases as B increases. Meanwhile, as the degree of anisotropic ω_y/ω_x increases at fixed ω_x the ratio also decreases.

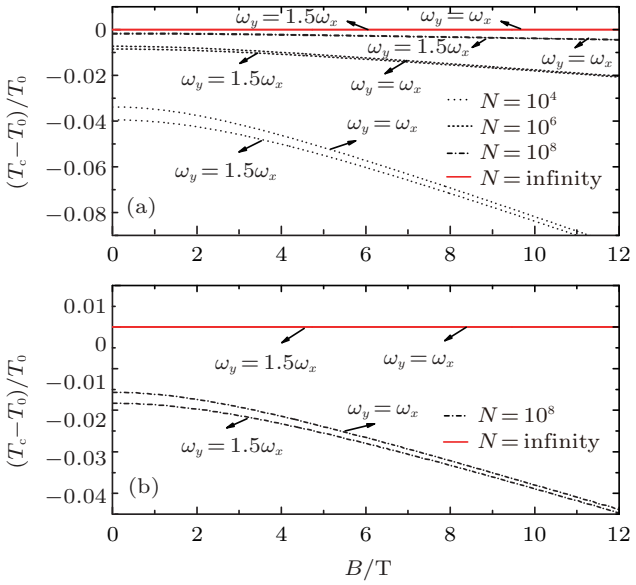


Fig. 3. (color online) (a) The $(T_{\rm c}-T_0)/T_0$ as a function of the strength of the magnetic field B for $\omega_x = \omega_y$ and $\omega_y = 1.5\omega_x$. We set $N = 10^4, 10^6, 10^8, \infty$ and $\omega_x = \omega_z = 10^3$ Hz in the plots. In order to see the $N = 10^8$ curve in panel (a) clearly, we replot it in panel (b) with a different vertical scale.

Next, let us examine the condensate fraction, i.e., the ratio of the number of condensate particles to the total particle number for $T < T_{\rm c}$. Since $N_0 \gg 1$ in this case, we may substitute $z \approx 1$ in Eq. (26) to obtain

$$\frac{N_0}{N} = 1 - \left(\frac{k_{\rm B}T}{\hbar\bar{\omega}_{\rm g}}\right)^3\frac{\zeta(3)}{N} - \gamma\left(\frac{k_{\rm B}T}{\hbar\bar{\omega}_{\rm g}}\right)^2\frac{\zeta(2)}{N}, \tag{33}$$

or using the expression for T_0 of Eq. (31), the above equation can be rewritten as

$$\frac{N_0}{N} = 1 - \left(\frac{T}{T_0}\right)^3 - \gamma\frac{\zeta(2)}{\zeta(3)^{2/3}}\left(\frac{T}{T_0}\right)^2 N^{-1/3}. \tag{34}$$

A plot of N_0/N as a function of (T/T_0) for different fixed values of the strength of the magnetic field B and particle number

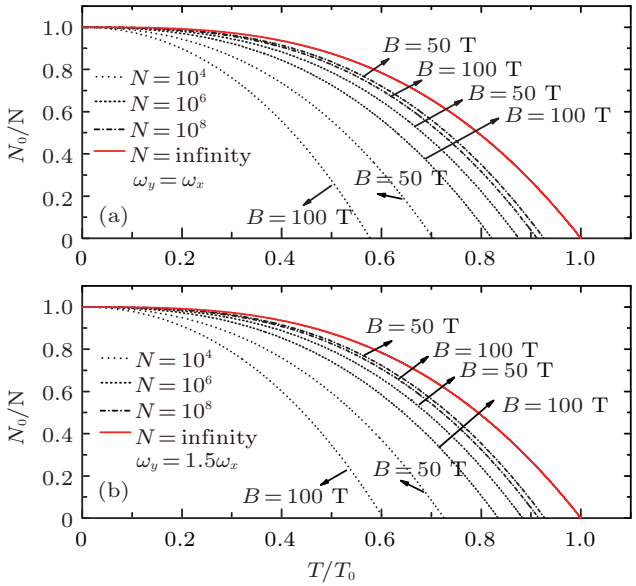


Fig. 4. (color online) The N/N_0 as a function of T/T_0 for different values of $B = 50$ T, 100 T or $\omega_c = 29.606$ kHz, 59.212 kHz, and $N = 10^4, 10^6, 10^8, \infty, \omega_x = \omega_z = 10^3$ Hz. In panel (a) we set $\omega_y = \omega_x$, and $\omega_y = 1.5\omega_x$ in panel (b).

N is given in Fig. 4. It is interesting to note that, in the case when $N \to \infty$, equation (34) reduces to

$$\frac{N_0}{N} = 1 - \left(\frac{T}{T_0}\right)^3,$$

thus the change of the B will not affect N_0/N. While in the finite particle number case, it is evident that when the value of B increases or N decreases, the value of N_0/N will be lowered as shown in Fig. 4. In order to make the curves distinguishable, we set $B = 50$ T, 100 T in the graphs.

3.3. Chemical potential

In this subsection, we investigate the chemical potential μ, or equivalently $z = e^{\beta(\mu - E_0)}$. Since it is clear when $T \le T_c$, $\mu = E_0$, we only need to find out μ when $T > T_c$. As discussed earlier, $N_0 = 0$ when $T > T_c$, hence, equation (26) can be rewritten as

$$N = \left(\frac{T}{T_0}\right)^3 \frac{N}{\zeta(3)} g_3(z) + \gamma \left(\frac{T}{T_0}\right)^2 \left(\frac{N}{\zeta(3)}\right)^{2/3} g_2(z), \quad (35)$$

which cannot be solved analytically. In order to obtain z as a function of (N, B, T), we solved Eq. (35) numerically and plot z and μ as functions of the temperature T/T_0 for different values of the B and N in Figs. 5 and 6. From the graphs, it is clear that in the region $T > T_c$, z and μ die down very fast as T increases. As shown in Fig. 6, μ dies down faster as the particle number increases.

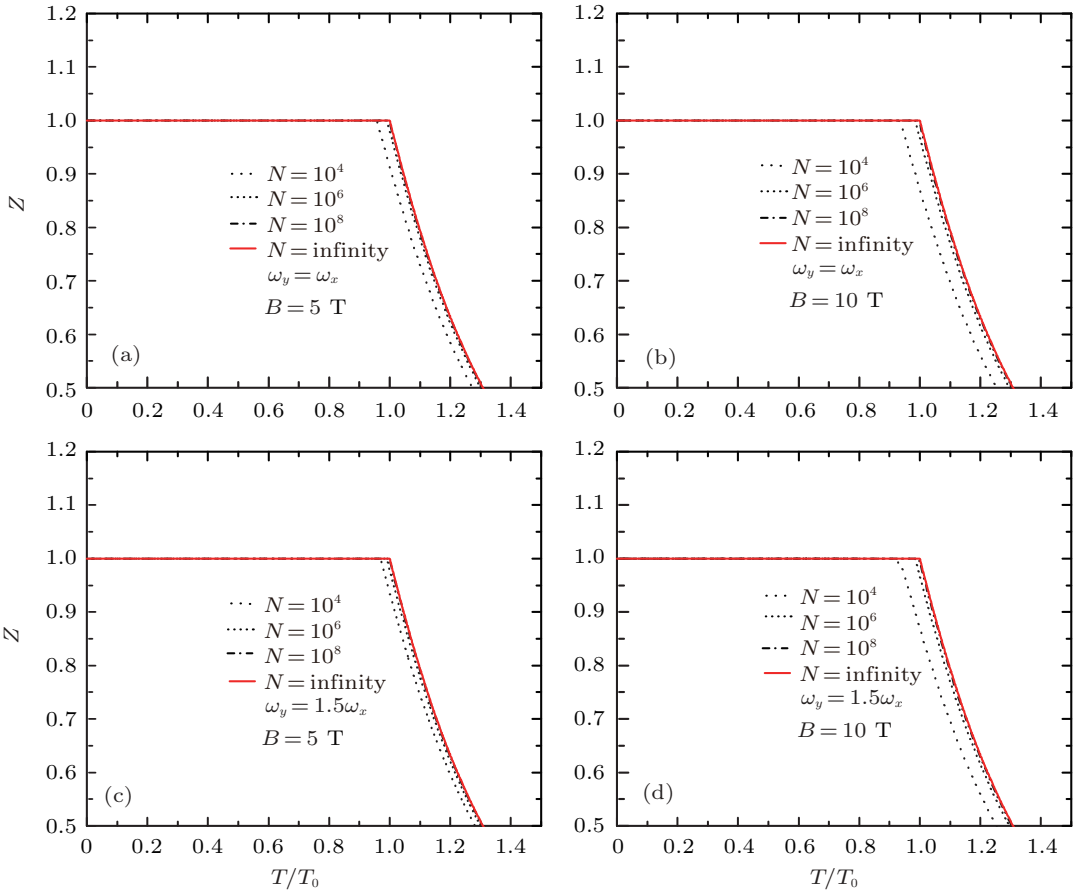


Fig. 5. (color online) The z as a function of T/T_0 for different values of $B = 5$ T, 10 T or $\omega_c = 2.9606$ kHz, 5.9212 kHz, $N = 10^4, 10^6, 10^8, \infty$, and $\omega_x = \omega_z = 10^3$ Hz. We set $\omega_y = \omega_x$ in panels (a) and (b) and $\omega_y = 1.5\omega_x$ in panels (c) and (d).

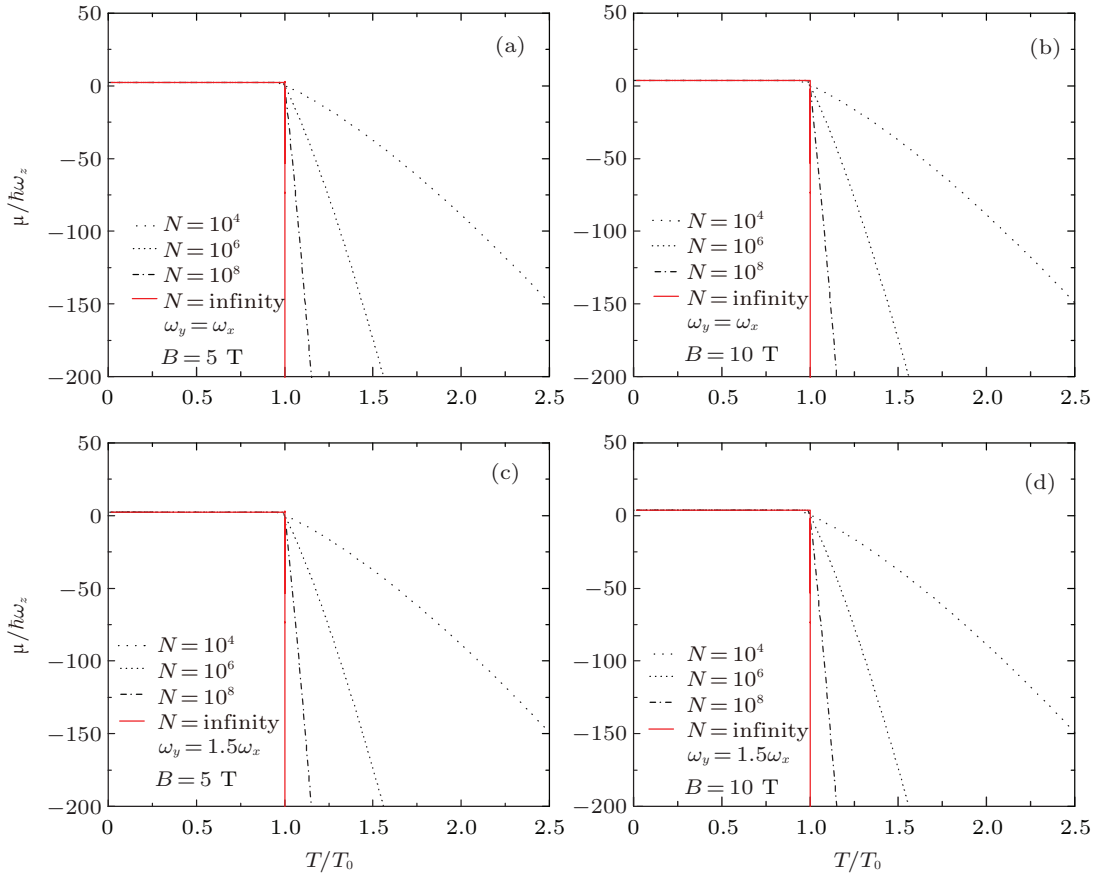


Fig. 6. (color online) Chemical potential μ as a function of T/T_0 for different values of $B=5$ T, 10 T and $N=10^4,10^6,10^8,\infty$, $\omega_x=\omega_z=10^3$ Hz. We set $\omega_y=\omega_x$ in panels (a) and (b) and $\omega_y=1.5\omega_x$ in panels (c) and (d).

In the thermodynamic limit $N\gg 1$, we can ignore the last term of Eq. (35). Therefore, when $T>T_c$ we have

$$z=\mathrm{e}^{\beta(\mu-E_0)}=g_3^{-1}\left[\frac{\zeta(3)}{\left(\frac{T}{T_0}\right)^3}\right], \tag{36}$$

where $g_3^{-1}[z]$ is the inverse function of $g_3(z)$. From Eq. (36), it is easy to obtain that

$$\mu(N,B,T)=E_0+k_BT\ln\left(g_3^{-1}\left[\frac{\zeta(3)}{\left(\frac{T}{T_0}\right)^3}\right]\right). \tag{37}$$

From Fig. 5, we note that in the regime $T>T_c$, only when $N_0=0$, $z=N_0/(N_0+1)\ll 1$ and $g_3(z)\approx z=\mathrm{e}^{\beta(\mu-E_0)}$, equation (37) reduces to $\mu\approx E_0-3k_BT\ln(T/T_0)$. However, there exists a transition region where the approximation $z\ll 1$ is not valid, then we have to use Eq. (37) to obtain the value of μ.

3.4. Specific heat

In this subsection we calculate the specific heat. The specific heat can be calculated by differentiating the internal energy U with respect to the temperature $C_v(T)=\partial U/\partial T$. The internal energy is given by

$$\begin{aligned}U&=\int_{E_0}^{\infty}\frac{\varepsilon}{\mathrm{e}^{\beta(\varepsilon-\mu)}-1}g(\varepsilon)\mathrm{d}\varepsilon\\&=NE_0+\int_0^{\infty}\frac{\varepsilon g(\varepsilon)}{\mathrm{e}^{\beta(\varepsilon-\mu)}-1}\mathrm{d}\varepsilon\\&=NE_0+\frac{3(k_BT)^4}{(\hbar\bar{\omega}_g)^3}g_4(z)+\frac{2\gamma(k_BT)^3}{(\hbar\bar{\omega}_g)^2}g_3(z).\end{aligned} \tag{38}$$

When $T\le T_c$, then $z\approx 1$ and the above equation reduces to

$$U=NE_0+\frac{3(k_BT)^4}{(\hbar\bar{\omega}_g)^3}\zeta(4)+\frac{2\gamma(k_BT)^3}{(\hbar\bar{\omega}_g)^2}\zeta(3), \tag{39}$$

thus the specific heat blow T_c is

$$\begin{aligned}\frac{C_{v<}}{Nk_B}&=\frac{12(k_BT)^3}{(\hbar\bar{\omega}_g)^3}\frac{\zeta(4)}{N}+\frac{6\gamma(k_BT)^2}{(\hbar\bar{\omega}_g)^2}\frac{\zeta(2)}{N}\\&=12\frac{\zeta(4)}{\zeta(3)}\left(\frac{T}{T_0}\right)^3+\frac{6\gamma\zeta(3)^{1/3}}{N^{1/3}}\left(\frac{T}{T_0}\right)^2.\end{aligned} \tag{40}$$

When $T>T_c$, the specific heat can be obtained from Eq. (38) directly,

$$\begin{aligned}\frac{C_{v>}}{Nk_B}&=12\left(\frac{T}{T_0}\right)^3\frac{g_4(z)}{\zeta(3)}+\frac{6\gamma}{N^{1/3}}\left(\frac{T}{T_0}\right)^2\frac{g_3(z)}{\zeta(3)^{2/3}}\\&\quad+\left[3\left(\frac{T}{T_0}\right)^4\frac{g_3(z)}{\zeta(3)}+\frac{2\gamma}{N^{1/3}}\left(\frac{T}{T_0}\right)^3\frac{g_2(z)}{\zeta(3)^{2/3}}\right]\frac{T_0}{z}\frac{\partial z}{\partial T}.\end{aligned} \tag{41}$$

We plot the specific heat as a function of T/T_0 for different values of B and N in Fig. 7. It is clear from the graphs that when N is finite, the specific heat exhibits a continuous change. While in the limit of $N \to \infty$, $T_c = T_0$, the specific heat shows an almost discontinuous jump at the transition temperature. When the particle number decreases, the maximum value of the specific heat decreases, and the whole curve moves left as the value of T_c decreases.

3.5. Magnetization

Similarly, the magnetization can be obtained from the thermodynamic potential

$$M = -\frac{\partial \Omega}{\partial B}\bigg|_{\mu,V,T}.$$

Hence, when $T < T_c$, it has two parts

$$M_< = M_0 + M_T, \tag{42}$$

where

$$M_0 = -\frac{\partial \Omega_0}{\partial B} = -N_0 \frac{\partial E_0}{\partial B},$$
$$M_T = -\frac{\partial \Omega_{T\neq 0}}{\partial B} = -N_e \frac{\partial E_0}{\partial B} + \frac{1}{\beta}\frac{(k_B T)^2 g_3(z)}{(\hbar\bar{\omega}_g)^2}\frac{\partial \gamma}{\partial B}. \tag{43}$$

Since $z \approx 1$ when $T < T_c$, equation (42) becomes

$$M_< \approx -N\frac{\partial E_0}{\partial B} + \frac{1}{\beta}\frac{(k_B T)^2 \zeta(3)}{(\hbar\bar{\omega}_g)^2}\frac{\partial \gamma}{\partial B}, \tag{44}$$

or equivalently,

$$\frac{M_<}{N} \approx -\frac{\partial E_0}{\partial B} + \frac{\partial \gamma}{\partial B}\left(\frac{T}{T_0}\right)^3 (\hbar\bar{\omega}_g). \tag{45}$$

The magnetization for $T > T_c$ can also be obtained readily

$$M_> = -N\frac{\partial E_0}{\partial B} + \frac{1}{\beta}\frac{(k_B T)^2 g_3(z)}{(\hbar\bar{\omega}_g)^2}\frac{\partial \gamma}{\partial B}, \tag{46}$$

or

$$\frac{M_>}{N} \approx -\frac{\partial E_0}{\partial B} + \frac{\partial \gamma}{\partial B}\left(\frac{T}{T_0}\right)^3 \frac{g_3(z)}{\zeta(3)}(\hbar\bar{\omega}_g). \tag{47}$$

The magnetization M as functions of T/T_0 for different values of B and N is plotted in Fig. 8. As clearly reflected in the graphs, the magnetization M varies with the temperature and the diamagnetism is stronger at lower temperatures. This result is different from those obtained in Ref. [24], their magnetization stays invariant at all temperatures. Actually, if one takes the thermodynamic limit $N \to \infty$, then the second terms in Eqs. (44) and (46) can be dropped and we would obtain the result that magnetization remains invariant at all temperatures.

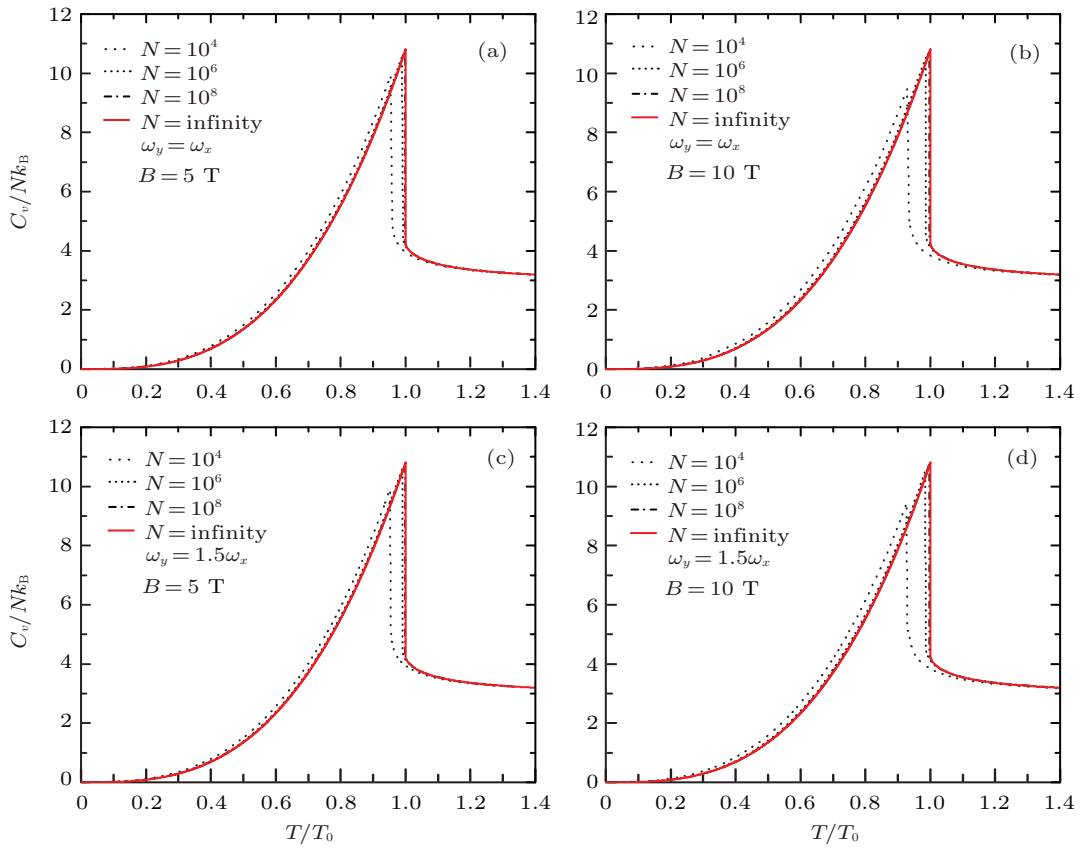


Fig. 7. (color online) The $C_v/(Nk_B)$ as a function of T/T_0 for different values of $B = 5$ T, 10 T, $N = 10^4, 10^6, 10^8, \infty$, and $\omega_x = \omega_z = 10^3$ Hz. We set $\omega_y = \omega_x$ in panels (a) and (b) and $\omega_y = 1.5\omega_x$ in panels (c) and (d).

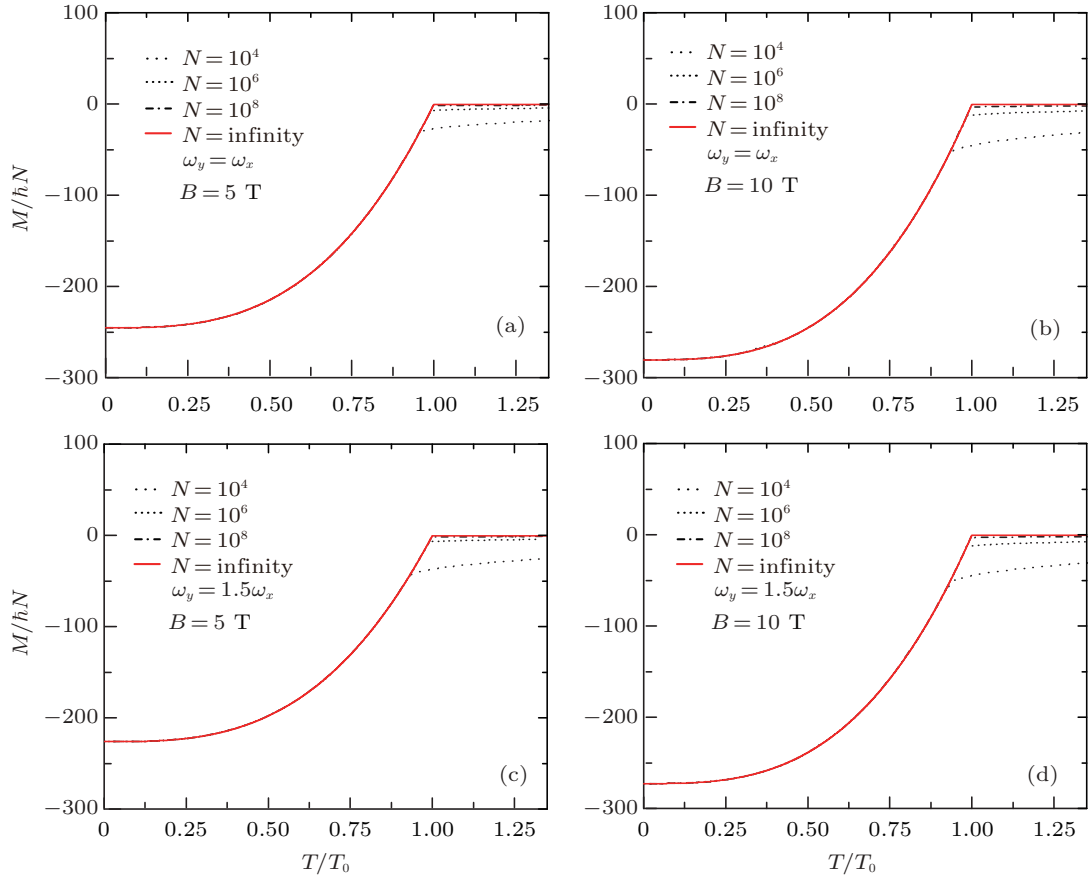


Fig. 8. (color online) Magnetization M as a function of T/T_0 for different values of $B=5$ T, 10 T, and $N=10^4, 10^6, 10^8, \infty$, $\omega_x=\omega_z=10^3$ Hz. We set $\omega_y=\omega_x$ in panels (a) and (b) and $\omega_y=1.5\omega_x$ in panels (c) and (d).

From the expressions above, we can see that the magnetization M does depend on B, since $\partial\gamma/\partial B\neq 0$. This point is clearly reflected in Fig. 8. Moreover, magnetization above T_c is different from that below T_c, this is different from the results in Ref. [24]. Actually this difference originated from Eq. (30), where we have kept the $N^{2/3}$ term, i.e. this is due to the finiteness of the particle number.

First, M/N as a function of T/T_0 (Eqs. (44) and (47)) appears to be the same for any value of particle number N. However, since the transition temperature depends on N, they are different for different values of N. It is worth stressing that M/N is a smooth function at T_c when $N\to\infty$, this is quite different from the specific heat curve. On the other hand, from Eqs. (45) and (47), we know that M vanishes as B reduces to zero at all temperatures implying that Meissner–Ochsenfeld effect does not exist in an anisotropic harmonically trapped CBG. This result agrees with those obtained in Ref. [24].

4. Conclusions

In summary, by employing an accurate density of states, we calculate analytically the thermodynamic potential of an ideal charged Bose gas confined in an anisotropic harmonic potential and a constant magnetic field. Then we obtained the expressions for the Bose–Einstein transition temperature, condensate fraction, the specific heat and magnetization taking into account the fact that the particle number N is finite. These thermodynamic properties are then investigated for different values of particle number N, strength of the magnetic field B, and different degrees of anisotropy for the confining harmonic potential. In contrast to the infinite number of particles case which has been investigated in Ref. [24], we show that those thermodynamic properties, in particular Bose–Einstein transition temperature, depends upon the strength of the magnetic field due to the finiteness of the particle numbers, and the collective effects of a finite number of particles become larger when the particle number decreases. Furthermore, the magnetization varies with the temperature due to the finiteness of the particle number while it stays invariant in the thermodynamic limit $N\to\infty$.

References

[1] Osborne M F M 1949 *Phys. Rev.* **76** 400
[2] Schafroth R 1955 *Phys. Rev.* **100** 463
[3] Dalfovo F, Giorgini S, Pitaevskii L and Stringari S 1999 *Rev. Mod. Phys.* **71** 463
[4] Inguscio M, Stringari S and Weiman C E (eds.) 1999 *Bose–Einstein Condensation in Atomic Gases* (Amsterdam: IOS Press)
[5] Pethick C J and Smith H 2002 *Bose–Einstein Condensation in Dilute Gases* (Cambridge: Cambridge University Press)

[6] Pitaevskii L and Stringari S 2003 *Bose–Einstein Condensation* (Oxford: Clarendon)

[7] Leggett A J 2006 *Quantum Liquids: Bose Condensation and Cooper Pairing in Condensed-Matter Systems* (New York: Oxford University Press)

[8] May R M 1959 *Phys. Rev.* **115** 254

[9] May R M 1965 *J. Math. Phys.* **6** 1462

[10] Toms D J 1995 *Phys. Lett. B* **343** 259

[11] Kirsten K and Toms D J 1997 *Phys. Rev. D* **55** 7797

[12] Rojas H P 1996 *Phys. Lett. B* **379** 148

[13] Daicic J and Frankel N E 1997 *Phys. Rev. B* **55** 2760

[14] Bayindir M and Tanatar B 2001 *Physica B* **293** 283

[15] van Zyl B P and Hutchinson D A W 2004 *Phys. Rev. B* **69** 024520

[16] Jean D, Fabrice G, Gediminas J and Patrik Ö 2011 *Rev. Mod. Phys.* **83** 1523

[17] Fetter A L 2009 *Rev. Mod. Phys.* **81** 647

[18] Stringari S 1999 *Phys. Rev. Lett.* **82** 4371

[19] Kling S and Pelster A 2007 *Phys. Rev. A* **76** 023609

[20] Balaž A, Vidanović I, Bogojević A and Pelster A 2010 *Phys. Lett. A* **374** 1539

[21] Li Y and Gu Q 2011 *Phys. Lett. A* **378** 1233

[22] Hassan A S, EI-Badry A M and Soliman S S M 2011 *Eur. Phys. J. D* **64** 465

[23] EI-Badry A M 2013 *Turk. J. Phys.* **37** 30

[24] Fan J H, Gu Q and Guo W 2011 *Chin. Phys. Lett.* **28** 060306

[25] Anderson M H, Ensher J R, Matthews M R, Wieman C E and Cornell E A 1995 *Science* **269** 198

[26] Davis K B, Mewes M O, Andrews M R, van Druten N J, Durfee D S, Kurn D M and Ketterle W 1995 *Phys. Rev. Lett.* **75** 3969

[27] Grossmann S and Holthaus M 1995 *Phys. Lett. A* **208** 188

[28] Ketterle W and van Druten N J 1996 *Phys. Rev. A* **54** 656

[29] Kirsten K and Toms D J 1996 *Phys. Rev. A* **54** 4188

[30] Haugerud H, Haugest T and Ravndal F 1997 *Phys. Lett. A* **225** 18

[31] Pathria R K 1998 *Phys. Rev. A* **58** 1490

[32] Lin M, Chen L, Chen J, Yan Z and Chen C 1999 *Phys. Rev. A* **60** 4168

[33] Klünder B and Pelster A 2009 *Eur. Phys. J. B* **68** 457

[34] Wang J H and Ma Y L 2010 *Chin. Phys. B* **19** 050502

[35] Xu Y, Jia D J, Li Z X, Hou F C, Tan L and Zhang L Y 2009 *Acta. Phys. Sin.* **58** 55 (in Chinese)

[36] Haugest T, Haugerud H and Andersen J O 1997 *Phys. Rev. A* **55** 2922

[37] Dippel O, Schmelcher P and Cederbaum L S 1994 *Phys. Rev. A* **49** 4415

[38] Pathria R K and Beale P D 2011 *Statistical Mechanics* (Boston: Academic) pp. 179–223

[39] Toms D J 1997 *Field Theoretical Methods in Fundamental Physics* (Seoul: Choonkyu Lee Mineumsa) pp. 17–107

[40] Standen G B and Toms D J 1999 *Phys. Rev. E* **60** 5275